DIRECTIONAL MEASUREMENTS AND MODELLING OF INDOOR ENVIRONMENTS AT 5.2GHZ

D.I. Laurenson[*]*, C.M. Tan*[†]*, C.C. Chong*[*] *and M.A. Beach*[†]

[*]Institute for Digital Communications, School of Engineering and Electronics
The University of Edinburgh, Mayfield Road, Edinburgh, U.K., EH9 3JL
[†]Centre for Communication Research, Electrical Engineering
University of Bristol, Bristol, U.K.
phone: + (44) 131 650 5579, fax: + (44) 131 650 6554, email: Dave.Laurenson@ed.ac.uk
phone: + (44) 117 954 5190, fax: + (44), email: M.A.Beach@bristol.ac.uk
web: www.mobilevce.com

ABSTRACT

State of the art antenna array systems require detailed information about the channel in order to maximise usable capacity. Such systems require both detailed analysis and realistic simulation based testing. To date there has been little work carried out in the area of directional channel characterisation when one of the terminals is in motion. This paper will describe a dynamic measurement campaign, conducted at Bristol University, employing antenna arrays, both for a SIMO configuration with a ULA, and a MIMO configuration employing CUBAs. Associated with the SIMO measurements, a modelling strategy was developed for simulating directional multipath propagation. The model is based on stochastic processes controlling the birth and death of observable multipath components, the temporal and spatial correlation of multipath components, the variation of the spatial and temporal properties of components as the terminal moves, and the spectral characteristics of these components. The generic framework is fitted to the measurements obtained, and the resulting parameters are presented.

1. INTRODUCTION

Radio channel measurement and modelling have been key elements in the assessment of communication systems since the first hardware simulators appeared. They are no less important today, although the systems that they support are infinitely more complex than those produced decades ago. Currently, the research focus is on directional channel models that may or may not incorporate the dynamic evolution of the environment. Such models are essential for assessing the potential of smart antenna based systems – key elements for support of high bandwidth communication.

In recent years, many studies have been conducted in order to gain a more detailed knowledge of radio propagation. Numerous channel models have been reported in the literature [1], [2]. A major shortcoming of many of these is that they do not consider dynamic behaviour of the channels, concentrating instead on a statistically stationary description of the channel. This can be attributed to the lack of dynamic measurement campaigns to support realistic modelling of a dynamic channel.

This paper describes work that has been carried out by Bristol University and The University of Edinburgh in the UK under the auspices of the Virtual Centre of Excellence in Mobile Communications (MobileVCE). Channel measurements were conducted by Bristol University, encompassing both dynamic SIMO and dynamic MIMO measurements, while the channel modelling work was carried out at The University of Edinburgh, principally focussing on the Dynamic SIMO data. Work to extend the model to the dynamic MIMO case is currently underway.

The remainder of the paper is organised as follows: Section 2 will describe the measurement equipment and operation, and section 3 the key parameters extracted from these measurements. Section 4 will introduce the modelling work, while section 5 will draw the paper to a close.

2. CHANNEL MEASUREMENTS

2.1 Measurement setup

Two sets of measurements were obtained for channel modelling purposes, a set of single input multiple output (SIMO) measurements, and a set of multiple input multiple output (MIMO) measurements. Both sets were conducted using a Medav RUSK BRI channel sounder operating at 5.2 GHz [3]. A periodic multitone signal with a bandwidth of 120 MHz and repetition period of 0.8 μs was used. The frequency domain channel response was calculated online and stored on the sounder's hard disk for post-processing.

For the SIMO measurements, the mobile transmitter (TX) used an omni-directional antenna transmitting at an input power of +26 dBm with a stationary receiver (RX) comprising a uniform linear array (ULA). The ULA had 8 active dipole-like elements spaced by half a wavelength and 2 dummy elements at both ends to balance the mutual coupling effects. The effective azimuth visible range of the ULA was 120º.

For the MIMO measurements, two identical 16-element uniform circular arrays with dual-polarised (horizontal and vertical) stacked patch antenna elements were used for both the transmitter and receiver. For the measurements conducted, only the vertical polarisation was considered. The ideal radius of the circular arrays was found to be 1.28λ.

Spatial calibration of all array systems was carried out in an anaechoic environment prior to measurements being conducted.

The dynamic measurements were conducted by slowly pushing the TX towards the RX using a trolley and wireless telemetry equipment specially developed for this dynamic channel sounding exercise. The trolley had 2 odometers on the left and right wheels that enable precise logging of the distance moved. For the SIMO measurement campaign, the sounder was configured to record 20 snapshots consecutively for every 18 mm moved. A snapshot consists of 8 complex channel response measurements in the frequency domain across the 8-element ULA. For a multitone signal period of 0.8 μs, the time for recording a full SIMO snapshot was 12.8 μs [3]. Therefore, the total recording time of 1 Fast Doppler Block (FDB) was 256 μs, which was well within the coherence time of the channel and also the 2 ms Medium Access Control (MAC) frame of the HIPERLAN/2 standard. A FDB in this measurement consists of a block of 20 consecutive SIMO snapshots.

2.2 Measurement Environments

One set of measurements were conducted in a highly cluttered modern office environment with standard office furniture, wooden shelves (height 1.83 m) and metal cabinets (height 1.3/1.85 m) present. The tables were separated by soft boards (height 1.3/1.5 m). The floor was carpeted with aluminium backed floor tiles and the walls were brick and concrete. Other environments included a research laboratory with aluminium frame benches, an open foyer, and a corridor. Full details of all of the conducted measurement scenarios are given in [4]. For SIMO measurements, the mobile TX was pushed along the dotted path and the RX was fixed at a position labelled as "RX" (Figure 1). In the MIMO case, it is the TX which is fixed, and the RX is mobile (Figure 2). The height of the fixed end was 1.7/2.1/2.5/3.0 m (depending on ceiling height), while the height of the mobile was set to 1.7 m. The arrow indicates the orientation of the ULA broadside direction. Measurements were conducted during both normal office and out of office hours.

3. KEY PARAMETERS EXTRACTED FROM MEASUREMENTS

The channel model parameters are based upon data from the measurement campaigns described above. In order to use such data it is necessary to extract multipath component parameters from the data, and then to translate these into model parameters.

3.1 Multipath Channel Parameter Estimation

The super-resolution frequency domain Space-Alternating Generalised Expectation maximisation (FD-SAGE) algorithm is used to detect and estimate the the number of multipath components (MPCs) and the complex path gain, time-of-arrival (TOA) and angle-of-arrival (AOA) of each of these [5]. The channel parameters vary as a function of mobile displacement, thus a set of varying parameters is obtained from the measurement data. The FDB index, n, corresponds to the MT displacement where the separation between FDBs is equivalent to 18mm. The total number of FDBs, N, varies according to the total distance travelled by the trolley. Typically, N lies between 500 and 850.

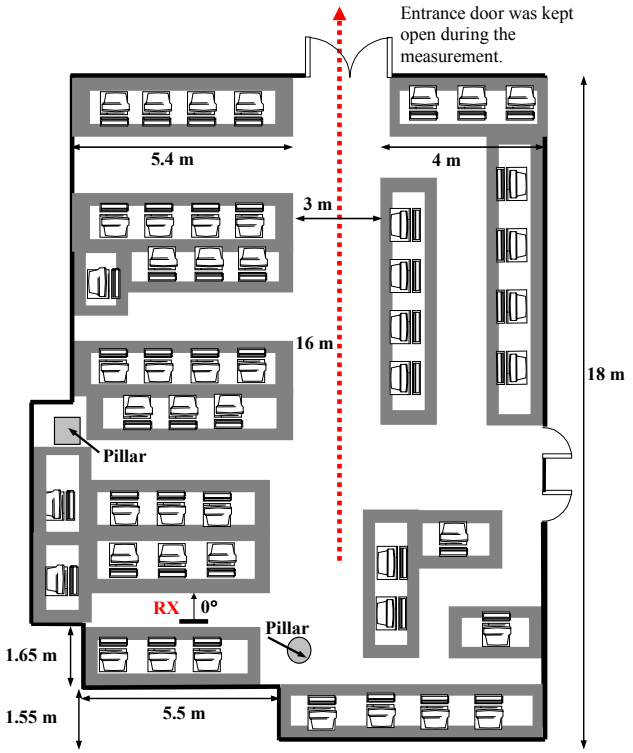

Figure 1: Office environment in SIMO configuration

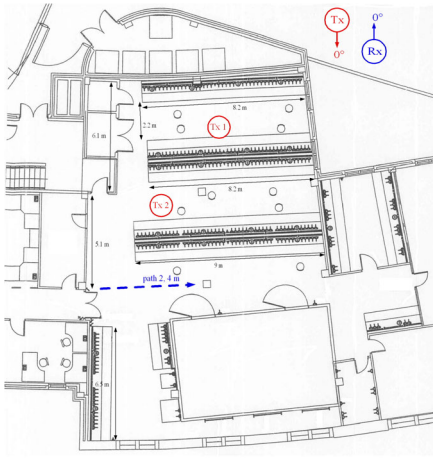

Figure 2: Research Laboratory in MIMO configuration

When dealing with the MIMO data, the added complication using the SAGE process is that its iterative nature does not scale well to the increased data size. In order to reduce the time required to perform the analysis, a hybrid-space SAGE (HS-SAGE) algorithm was developed [6].

3.2 Joint Parameter Estimation Results

Analysis of the joint parameter distributions was performed on the MIMO data. All array rotations were normalised in post-processing such that the transmitter and receiver 0º directions faced each other at all measurement positions.

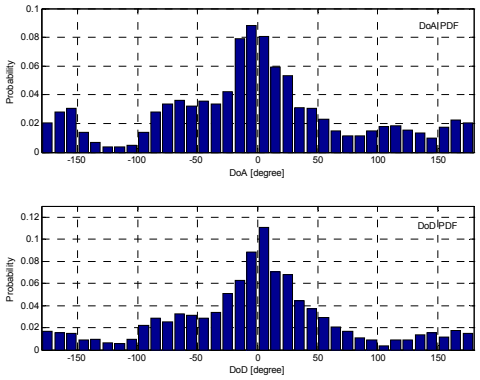

Figure 3: Aggregated direction of arrival (DoA) and direction of departure (DoD) distributions

The direction of departure and direction of arrival distributions are shown in Figure 3, and indicate that for the indoor environment studied, there is a bias for multipath components to appear around the 0º angle. This would indicate that despite the clutter, an assumption of paths arriving equally from all angles is invalid for such environments.

Correlations between DoD and DoA can be observed when their joint distribution is plotted, as shown in Figure 4. The largest peak corresponds to the direct path between the transmitter and receiver, and there are also substantial peaks corresponding to back-wall reflections, appearing at angles of 180º. When the joint power density is considered (Figure 5), it becomes clear that not only are these directions the most commonly observed, but they also correspond to the most substantial contributions to overall received power.

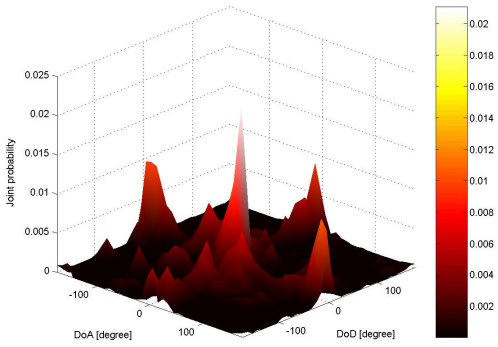

Figure 4: Joint distribution of DoD/DoA

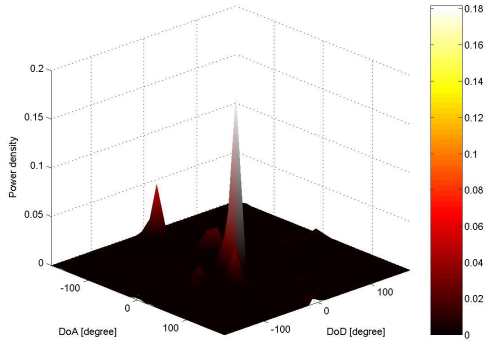

Figure 5: Joint power density DoD/DoA

3.3 Identification of Path "Birth" and "Death"

In order to model the dynamic nature of the channel, a birth death model is used to describe the distance varying nature of the multipath propagation. The active paths in each particular FDB can be classified as new or inherited paths. New paths or births are defined as paths that first appear in that particular FDB, while inherited paths are defined as paths that existed in the previous FDB. A death is defined as an inherited or new path that does not appear in the next FDB.

In order to identify the number of births, L_B, and deaths, L_D, in each FDB, we introduced the terms active path (AP), active region (AR) and uncertainty region (UR). The area of the AR is determined by the intrinsic temporal and angular resolution of the measurement system, namely the Rayleigh resolution [7]. Here, the temporal and spatial coverage area of the AR is set to be $\tau_A \pm \delta\tau$ and $u_A \pm \delta u$, respectively, where τ_A and u_A (the spatial domain here is expressed in u-space, defined as $u = \sin\phi$) form the centroid of the AR, while $\delta\tau$ and δu are chosen to be 9ns and 0.25, respectively.

Multipath components may exist in one FDB, disappear for one or more FDBs, and then reappear. The temporary disappearance of these paths may be due to the fact that they are in a deep fade position, i.e. a null in the resultant complex path gain of the cluster. Thus, if paths appear, disappear and reappear within a finite local region, they can still be assumed to be within their lifespan. A distance of three wavelengths was chosen as a reasonable range within which to consider that a multipath component may be in a deep fade.

4. DYNAMIC CHANNEL MODEL

The channel model comprises two key components, a static directional component that describes the location of multipath components in delay and angular space, and a dynamic component that models the behaviour of these componentts over time.

4.1 Static model

The measured time and angle of arrival of multipath components were found to form clusters in the spatio-temporal domain [8]. These were analysed using joint distribution functions, an example of which is shown in Figure 6. On average, 9 clusters were identified in the office environments, and within these clusters, the number of multipath components is approximated by an exponential distribution, with clusters typically having fewer than five multipath components.

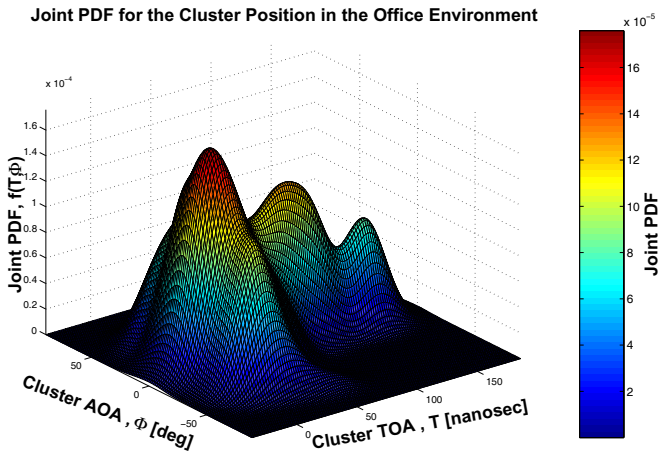

Figure 6: Joint PDF of cluster position in the office environment.

By employing two joint PDFs to describe multipath component location in the spatio-temporal domain, a two stage process results. The correlation between the spatial and temporal domains is described by the joint PDF of cluster position, $f(T_k,\Phi_k)$, and the joint PDF of MPCs position within a cluster, $f(\tau_{kl},\phi_{kl})$.

Using the Anderson-Darling goodness-of-fit test, the cluster position PDF is found to be described by an exponential distribution for the delay, and a Gaussian distribution in angle. Thus

$$f(T_k)=\begin{cases}\frac{1}{\mu_T}\exp\left(-\frac{T_k}{\mu_T}\right), & T_k>0\\ 0, & otherwise\end{cases}$$

and

$$f(\Phi_k \mid T_k)=\frac{1}{\sqrt{2\pi}\cdot\sigma_{\Phi|T}}\exp\left\{-\frac{(\Phi_k-\mu_{\Phi|T})^2}{2\sigma^2_{\Phi|T}}\right\}.$$

The mean, $\mu_{\Phi|T}$ of $f(\Phi_k|T_k)$ was constant at 0° (i.e. the LOS direction) while the standard deviation, $\sigma_{\Phi|T}$, for line of sight environments, varies according to a Weibull distribution,

$$\sigma_{\Phi|t_n}(t_n)=c_{\Phi|t_n}\cdot\left(\frac{t_n}{a_{\Phi|t_n}}\right)^{b_{\Phi|t_n}-1}\cdot\exp\left[-\left(\frac{t_n}{a_{\Phi|t_n}}\right)^{b_{\Phi|t_n}}\right],$$

where the parameters are found using non-linear regression.

Within the clusters the joint PDF, $f(\tau_{kl},\phi_{kl})$, is found to be separable with time of arrival again being described by an exponential distribution, but the angle of arrival being described by a Laplacian distribution,

$$f(\phi_{kl} \mid \tau_{kl})=\frac{1}{\sqrt{2}\sigma_{\phi|\tau}}\exp\left\{-\sqrt{2}\frac{|\phi_{kl}-\mu_{\phi|\tau}|}{\sigma_{\phi|\tau}}\right\}.$$

The parameters are detailed in Table 1 for line of sight (LOS), obstructed line of sight (OLOS) and non-line of sight (NLOS) environments.

Parameter	LOS	OLOS	NLOS
μ_T	40.9ns	41.2ns	52.9ns
$a_{\Phi\|tn}$	50.2		

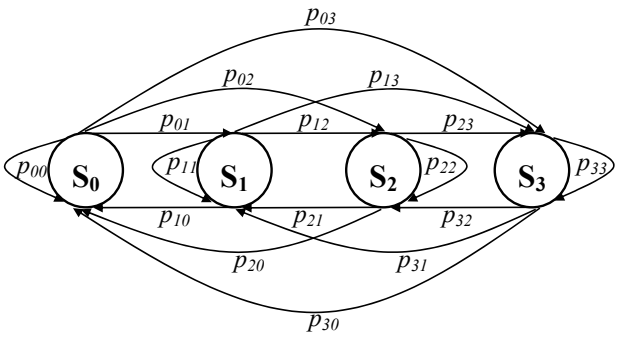

Figure 7: 4-state Markov model

Parameter	LOS	OLOS	NLOS
$b_{\Phi\|tn}$	1.54		
$c_{\Phi\|tn}$	67.7		
$\sigma_{\varphi\|T}$	3.9º	9.0º	7.3º
μ_t	13.8ns	22ns	33.4ns

Table 1: Static model parameters

4.2 Dynamic model

A 4-state Markov channel model (MCM) is proposed in order to model the dynamic evolution of paths when the MT in motion. At any time instant, the propagation channel can only be operating in one of the four possible states, where each of the state may be defined as follows:

- S0 – No "births" or "deaths"
- S1 – 1 "death" only
- S2 – 1 "birth" only
- S3 – 1 "birth" and 1 "death"

Four states are required in order to account for the correlation that exists between L_B and L_D. Figure 7 illustrates the state transition diagram of the 4-state MCM.

The transitions between states is defined by the probability matrix, **P**, given by

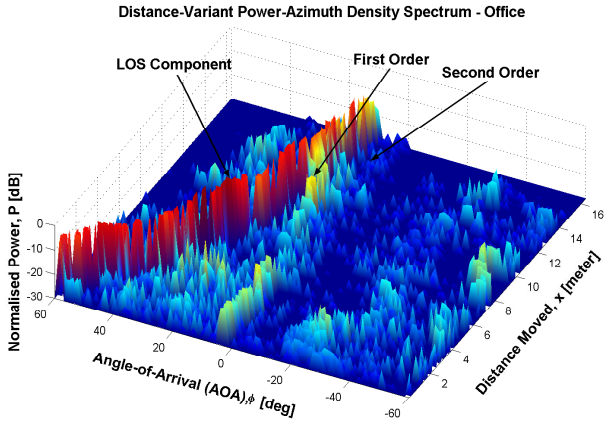

Figure 8: Distance-variant power-azimuth density spectrum (DV-PADS)

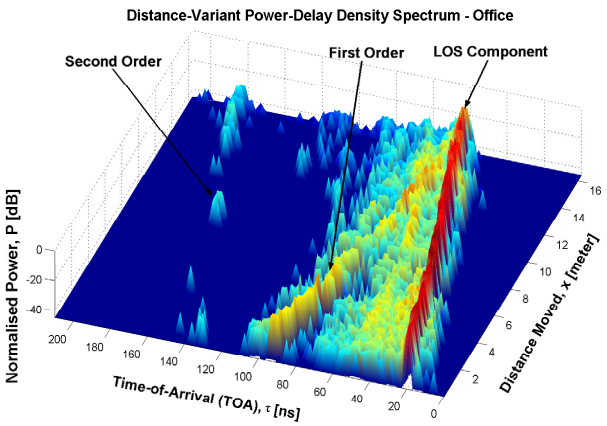

Figure 9: Distance-variant power-delay density spectrum (DV-PDDS)

$$\mathbf{P} = \{p_{ij}\} = \begin{pmatrix} p_{00} & p_{01} & p_{02} & p_{03} \\ p_{10} & p_{11} & p_{12} & p_{13} \\ p_{20} & p_{21} & p_{22} & p_{23} \\ p_{30} & p_{31} & p_{32} & p_{33} \end{pmatrix} \quad (1)$$

where i and j are state indices, and p_{ij} is the probability that a process currently in state i will occupy state j after its next transition.

Analysis of the measurement data shows that multiple births and deaths can occur between two consecutive FDBs. In order to account for this, a multiple step (M-step) MCM is proposed. By applying the 4-state MCM M times, both the correlation between L_B and L_D as well as multiple births and deaths will be achieved.

4.3 Model parameters

The measurement data were fitted to (1) through solving a set of 29 over-determined nonlinear equations. The resulting parameter set describes the 4-state MCM parameters required to generate a set of multipath births and deaths that have similar characteristics to the measured data itself. Figure 8 shows the distance-variant power-azimuth density spectrum (DV-PADS) and Figure 9, the distance-variant power-delay density spectrum (DV-PDDS) for a sample measurement file. The DV-PDDS shows that the TOA of the strongest LOS component increases as the trolley moves along its trajectory, corresponding to the trolley moving away from the RX. Also observable in the graph are the higher order reflections. The major first order reflection is due to a reflection off the wall with the entrance door. This accounts for the decrease in TOA as the trolley moves further away from the RX. On the other hand, the major second order reflection is due to the signal being first reflected by the wall behind the RX (first order), and then reflected again by the wall with the entrance door (second order) before arriving at the RX.

The figure also illustrates the appearance and disappearance of multipath components in the angular temporal plane. In general, larger values of L_B and L_D were obtained for the OLOS and NLOS scenarios when compared to the LOS scenario. This is mainly due to a larger total number of multipath components in OLOS and NLOS environments. The presence of a LOS path causes the channel sounder to miss paths with relatively low powers as the dynamic range of the channel sounder is finite (i.e. 40 dB). As diffuse reflections dominate in the OLOS and NLOS scenarios, the strongest paths detected by the channel sounder have approximately the same power. Therefore, paths with relatively low power can still be detected by the channel sounder provided they fall within the dynamic range.

Under the LOS condition, $M = 3$ is sufficient, while for the OLOS and NLOS cases, at least $M = 8$ is required in order to ensure **P** converges. These values were verified by simulation results by increasing M until the value of **P** did not change significantly. For example, under the LOS condition it was observed that all elements of **P** estimated at $M = 3$ and $M = 4$ (i.e. $\mathbf{P}_3$ and $\mathbf{P}_4$, respectively) do not vary by more than 15%. Increasing M further does not alter the value of **P** significantly. Thus, $M = 3$ is used as the upper limit of the step size to generate **P** for the LOS case. A similar observation was made for the OLOS and NLOS cases where the difference between $\mathbf{P}_8$ and $\mathbf{P}_9$ is insignificant. Therefore, $M = 8$ is used as the upper limit of the step size for the OLOS and NLOS cases.

An assessment of the performance of this approach can be made by examining the total number of active paths for a

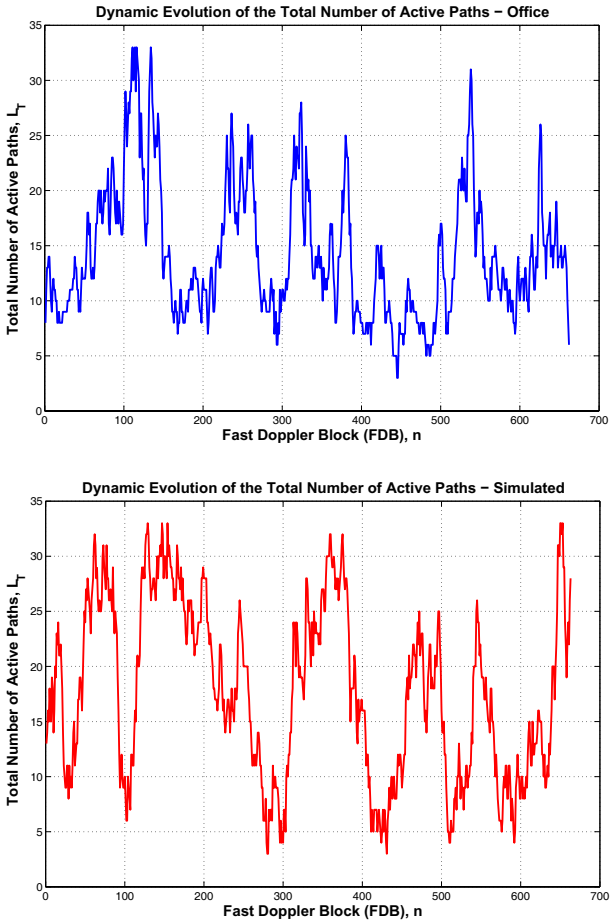

Figure 10: Total number of multipath components, measured and simulated

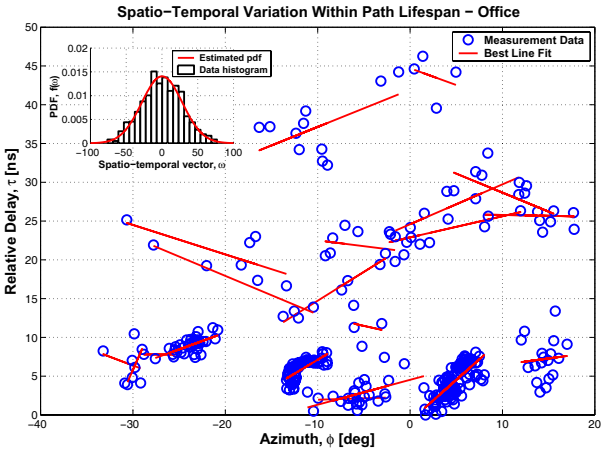

Figure 11: Variation of multipath component angle and time of arrival

given scenario. Figure 10 shows the number of paths detected in the measurement results, and a simulation using the Markov parameter set extracted from this measurement environment. Similar trends in the total number of multipaths can be observed in both measured results and in simulation results, indicating a certain degree of confidence that the non-linear optimisation has produced results that are representative of the practical environment.

4.4 Variation of multipath components within their lifespan

During the lifespan of a multipath component, its time of arrival, direction of arrival and power will vary due to motion in the environment. This is a key element of the dynamic nature of the channel, and will be different from the traditional Rayleigh fading based approaches, which are based upon the concept of multiple coincident multipath components.

In order to characterise the component variation, the measurement results were examined to find those multipath components that had the longest lifetimes. These could be used in the analysis process as their longevity contributed to more statistically significant data on how components vary over time.

Firstly, the time and angle of arrival were examined to determine how these varied jointly for a given multipath component: joint estimation is used as correlation between time of arrival and angle of arrival has already been established. Figure 11 shows a scatter plot of all of the long lived multipath components' parameters for an entire measurement run. With the knowledge of the FDB number for each of these points, the variation of a single multipath component can be identified. Drawn on this plot are the best fit lines indicating the direction of variation of multipath components in this spatio-temporal plane.

Using a definition of a spatio-temporal vector, ω, which describes the angle between the angle of arrival axis and the best line fit in Figure 11, a description of how multipath components vary can be defined. It is found that the spatio-temporal vector is not dependent upon time of arrival or angle of arrival, and is well modelled by a truncated Gaussian distribution, shown as an inset in Figure 10.

In order to model the power variation of a path within its lifespan, its power spectral density (PSD) is studied in order to determine an appropriate filter that is able to reproduce a set of random signals that exhibit the similar spectral characteristics. Figure 12 and Figure 13 illustrate the power variation of a single path selected from the measurement data and its corresponding PSD (in logarithmic scale), respectively. These figures show that only low frequency components are significant. Several other paths were also investigated and similar PSDs were observed. This implies that the power variation of path within its lifespan can be well-modelled by a simple LPF and a white noise source which exhibits a similar frequency response. The power variation of a path within its lifespan can be caused by several mechanisms. Firstly, due to the motion of the MT along its trajectory that changes the reflection coefficients of some media. For example, as the trolley moves along the trajectory in the office environment, reflections can be due to the walls, furniture, doors or even people in the surroundings. Thus, the building structure can cause a path to fade within its lifespan. Secondly, due to the finite spatio-temporal resolution of the measurement sys-

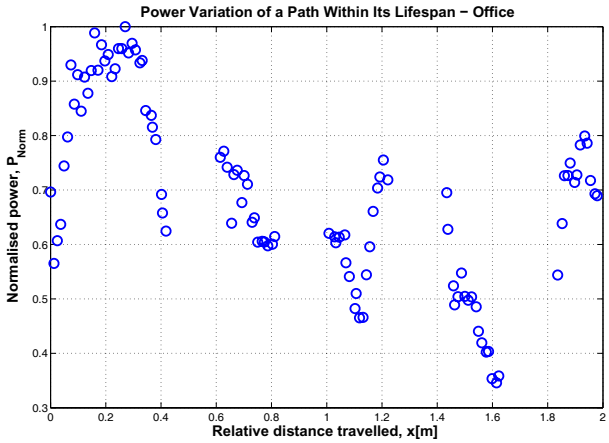

Figure 12: Power variation of a single multipath component

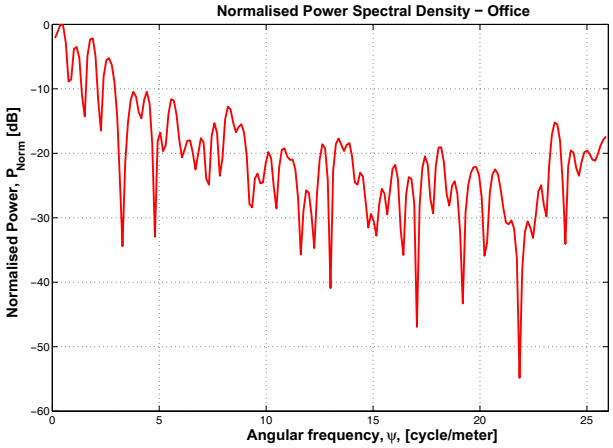

Figure 13: Power spectral density of a single multipath component

tem, paths with closely spaced TOAs and AOAs are unable to be resolved. This causes multiple paths being detected as "a single path" which will fade due to changes in path lengths of the unresolvable components.

4.5 Model implementation

Parameters suitable for an office environment for the Markov model are; for line of sight,

$$\mathbf{P_{LOS}} = \begin{pmatrix} 0.9039 & 0.0290 & 0.0367 & 0.0272 \\ 0.0000 & 0.5029 & 0.0000 & 0.4972 \\ 0.0000 & 0.0000 & 0.1663 & 0.8340 \\ 0.0000 & 0.3064 & 0.4165 & 0.2772 \end{pmatrix}$$

and for non-line of sight,

$$\mathbf{P_{NLOS}} = \begin{pmatrix} 0.9911 & 0.0029 & 0.0020 & 0.0018 \\ 0.0000 & 0.8869 & 0.0001 & 0.1131 \\ 0.0000 & 0.0000 & 0.5286 & 0.4715 \\ 0.0000 & 0.0000 & 0.9588 & 0.0411 \end{pmatrix}$$

Using these matrices, the *M*-step model can be run to produce birth-death statistics of multipath components. Parameters for new components are selected from the joint distribution functions defined for static environments, and their dynamic evolution defined from the spatio-temporal angle and power spectral density defined above. The resulting set of multipath components can then be used as a directional channel implementation as input to a system simulation

5. CONCLUSIONS

This paper has described a measurement and a modelling approach for producing detailed dynamic channel models that can be employed in antenna array based simulation systems. The measurement system produces data in a form that allows for joint distributions between angle of arrival, angle of departure and time of flight to be formulated, the resulting distributions being then used to create a channel model. MIMO measurements have indicated that there is strong correlation between angle of departure and angle of arrival of multipath components; this information should be incorporated into future channel models in order to better test practical system implementations. A channel modelling approach has been described, with data fitting it to SIMO measurements, showing how correlated time of arrival and angle of arrival information can be used to generate realisations of multipath channels.

6. ACKNOWLEDGEMENTS

The work reported in this paper has formed part of the Wireless Access area of the Core 2 Research Programme of the Virtual Centre of Excellence in Mobile & Personal Communications, Mobile VCE, www.mobilevce.com, whose funding support, including that of EPSRC, is gratefully acknowledged. Fully detailed technical reports on this research are available to Industrial Members of Mobile VCE. Chia Chin Chong would also gratefully acknowledge funding from a Vodafone Scholarship.

REFERENCES

[1] R. B. Ertel, P. Cardieri, K. W. Sowerby, T. S. Rappaport and J. H. Reed, "Overview of spatial channel models for antenna array communication systems," *IEEE Pers. Commun*., vol. 5, no. 1, pp. 10-22, Feb. 1998.

[2] U. Martin, J. Fuhl, I. Gaspard, M. Haardt, A. Kuchar, C. Math, A. F. Molisch and R. Thomä, "Model scenarios for direction-selective adaptive antennas in cellular mobile communication systems – scanning the literature," *Wireless Pers. Commun.*, vol. 11, no. 1, pp. 109-129, Oct. 1999.

[3] R. S. Thomä, D. Hampicke, A. Richter, G. Sommerkorn, A. Schneider, U. Trautwein and W. Wirnitzer, "Identification of time-variant directional mobile radio channels," *IEEE Trans. Instrum. Meas.,* vol. 49, no. 2, pp. 357-364, Apr. 2000.

[4] C. M. Tan, M. A. Beach and A. R. Nix, "Indoor dynamic SIMO measurement and samples of post-processed results," Internal report for Mobile VCE Core II WP3.1.1 Deliverable, Jan. 2002.

[5] C. C. Chong, D. I. Laurenson, C. M. Tan, S. McLaughlin, M. A. Beach and A. R. Nix, "Joint detection-estimation of directional channel parameters using the 2-D frequency domain SAGE algorithm with serial interference cancellation," in *Proc. IEEE Intl. Conf. Commun. (ICC 2002)*, New York, USA, Apr. 2002, pp. 906-910.

[6] C.M. Tan, M.A. Beach, and A.R. Nix, "Multipath parameters estimation with a reduced complexity unitary-SAGE algorithm," *European Transactions on Telecommunications,* Vol 14, pp. 515-528, January 2004.

[7] S. Haykin, *Adaptive Filter Theory*, 4th ed., New York: Prentice Hall, 2001.

[8] C. C. Chong, C. M. Tan, D. I. Laurenson, S. McLaughlin, M. A. Beach, A. R. Nix, "A New Statistical Wideband Spatio-Temporal Channel Model for 5GHz Band WLAN Systems", *IEEE J. Select. Areas Commun.*, vol. 21, no. 2, pp. 139-150, Feb. 2003.